Spring 5-1-2011

# Primary and Secondary Flow Structures in a Model Cerebral Aneurysm

Morgan A. Nowak

Follow this and additional works at: https://surface.syr.edu/honors_capstone

Part of the Other Aerospace Engineering Commons

# Primary and Secondary Flow Structures in a Model Cerebral Aneurysm


A Capstone Project Submitted in Partial Fulfillment of the
Requirements of the Renée Crown University Honors Program at
Syracuse University


Morgan A. Nowak

Candidate for B.S. Degree
and Renée Crown University Honors

6/2011


Honors Capstone Project in Aerospace Engineering


Capstone Project Advisor: _____
(Mark Glauser)

Honors Reader: _____
(John Dannenhoffer)



Honors Director:_____
James Spencer, Interim Director

Date:_____

ABSTRACT

Cerebral aneurysms affect 5% of western populations and can cause morbidity and mortality if they rupture. Various treatments can be used to minimize the risk of rupture, with new diagnostics and treatments under development that require information from non-invasive techniques such as Particle Imaging Velocimetery (PIV). The current study focused on developing a setup as a basis for future experiments and work on intracranial aneurysms involving PIV. PIV experimentation and data collection were carried out during the summer of 2010 at Ohta Labs of Tohoku University in Sendai, Japan. The experimental setup consisted of a pulsatile flow system, which was configured to realistically reproduce conditions found in cerebral aneurysms. PIV is often used as a validation measure in tandem with Computational Fluid Dynamic (CFD) research, and it is important that experimental setups in PIV produce realistic hemodynamics. A PIV system was used to record velocity field data in select planes through a silicone model of a curved artery with a saccular aneurysm attached at a 90 degree angle to the bend. Hemodynamics throughout the aneurysm and near aneurysm region of the parent artery were successfully recorded for future reference with CFD. Focal attributes to confirm experimental success were: 1) creation of laminar flow before the aneurysm; 2) development of Dean Vortices that interacted predictably with the aneurysm; and 3) aneurysmal inflow consistent with physiological data.

# TABLE OF CONTENTS

# LIST OF FIGURES

ACKNOWLEDGEMENTS

I appreciate the hard work and dedication all of the professors who worked on this project. Professor Hiroshi Higuchi (deceased Fall 2010; Syracuse University) and Professor Makoto Ohta (Tohoku University) provided me with invaluable knowledge and mentorship throughout the experimentation process, and greatly facilitated my Honors Thesis research work in Japan.

I am thankful that Professor Mark Glauser was able to help me bring this project to a close and guide the completion of my Capstone project. I appreciate that Professor John Dannenhoffer was able to be the Reader for this Honors Thesis.

Members of Professor Higuchi's lab in Syracuse and Ohta Labs in Tohoku were invaluable to my research experience. They created a friendly atmosphere which made working with them a joy.

Syracuse University and its Mechanical and Aerospace Engineering Department and Research Experience for Undergraduates, Tohoku University, and the Renée Crown Honors Program at SU provided numerous learning and work opportunities, which made my undergraduate education and the formation of this Capstone project enjoyable, full and informative. I am appreciative to have had the support of all of the Honors Program staff including Vicki, Marilyn, Eric, Steve, Hanna, Carolyn and Blythe, who helped me get the most out of my undergraduate experience at Syracuse University.

Finally, my family deserves credit for keeping me from getting overwhelmed, supporting my plans, and encouraging me to finish my Capstone project --  especially my father, who committed a lot of time and interest into this endeavor.  Without his help and encouragement this Capstone project would not have been finished.

INTRODUCTION

An aneurysm is a condition where a section of arterial wall distends and balloons out due to a loss of structural integrity, allowing blood to flow from the artery into the resultant peripheral cavity (Waite and Fine 2007). Generally found on arteries in the abdomen or in the brain, aneurysms often arise when a weakness develops in the tunica media, the muscle layer of the arterial wall. Estimates of cerebral aneurysm prevalence in western populations have been as high as 5% (ISUIA 1998). Cerebral aneurysms, also known as saccular-type, are generally smaller and more spherical in shape than those found elsewhere in the body (e.g., those commonly found in the abdominal cavity). Eventually, there is a risk that an aneurysm may rupture, causing uncontrolled internal bleeding (Brisman et al. 2006).  When this occurs in a cerebral aneurysm, a severe headache develops, associated with sub-arachnoid hemorrhaging and requiring immediate medical attention. Severe complications, including hydrocephalus and cerebral vasospasm, can occur, which have a high morbidity and mortality rate.

Several procedures can be applied as attempts to prevent aneurysm growth and rupture, most involving efforts to reduce blood flow through the aneurysm (Chen et al. 2004). Reduced flow may cause thrombosis to occur, resulting in the formation of a blood clot within the aneurysm that prevents further blood flow into it. This is often accomplished by placement of a stent across the aneurysm orifice or filling

the aneurysm with coils, known as coil embolization. Surgery carries a morbidity rate that can be as high as 10%. Doctors must carefully weigh the risk of aneurysm rupture with the risk of surgery when diagnosing an aneurysm and prescribing treatment. Non-invasive diagnostics tests and experimental tests of treatment procedures have been developed to learn how and when to treat aneurysms.

Histological studies looking at factors such as age, blood pressure, and smoking habits have failed to provide statistically significant risk factors associated with aneurysm rupture (Juvela 2003). A large portion of diagnosing has turned to the analysis of aneurysm flow models, which show promise in being used to predict aneurysm growth (Shimogonya et al. 2009), risk of rupture (Cebral et al. 2010), and how treatments may or may not reduce that risk (Baráth et al.2005). Common parameters of interest to researchers attempting to model aneurysm dynamics and diagnosis are associated with local hemodynamics, or characteristics of blood flow in and around the aneurysm (Cebral et al. 2010). There are a multitude of quantifiable flow effects that can be studied within the hemodynamics of an aneurysm, including velocity, pressure, vorticity, helicity, wall shear stress, oscillatory shear index, and various flow structures and characteristics. Since these parameters can be difficult and cost prohibitive to obtain through in vivo testing, various in vitro tests can be employed to model aneurysms.

A common method in obtaining experimental data on flow through a model aneurysm is Particle Imaging Velocimetry (PIV). PIV is a process in which particles are seeded into a fluid flow and illuminated within planes by a laser sheet (Raffel et al. 1998). A high-speed digital camera is used to produce images of these particles. Computer software is used to analyze consecutive images and create a flow field based on the paths that groups of particles make within the flow. With respect to aneurysm research, a PIV setup is produced by pumping a physiologically representative liquid through a clear model (usually a model of plexiglass or silicone) of an artery and aneurysm. PIV methods can be used to produce velocity field diagrams and various flow field effects, but not all parameters of interest in understanding aneurysms are available through PIV, e.g., it can be difficult to obtain accurate measures of wall shear stresses (Goldstein 1996).

Another, more recent method in obtaining data on flow through a model aneurysm is Computational Fluid Dynamics (CFD) (Taylor and Draney 2004). CFD is a process in which a computer-generated model is populated with a grid several hundred thousand cells in size (Versteeg and Malalasekra 2007). Initial conditions for the flow being studied are specified for the cells, such as incoming flow data, wall boundaries, and fluid properties. A program then updates each cell's properties based on the neighboring cells and a set of governing fluid dynamic equations. This cell updating is repeated over several thousand iterations until a

convergence in the solution is obtained and the cells no longer appreciably change.

With its computational basis, CFD can readily produce important flow parameters, such as wall shear stresses. It is also relatively easy to make small changes to a CFD model to assess how they might affect the overall flow pattern (Imai 2008), something that PIV cannot effectively do except with many different models, which can be cost prohibitive.

Yet, despite the power and cost effectiveness of CFD, PIV is still important in aneurysm research, and is commonly coupled with CFD to provide quality assurance and control; experimental data from PIV can be used to validate the calculations made with CFD. For example, CFD was coupled with PIV validation in a study of the effect of different radial positions of aneurysms on a curved parent artery (Liou et al. 2006). PIV validation of CFD with slight geometric variations showed that small variations can cause different flow effects; similar models can show qualitative similarities but have different quantitative parameters (Hoi et al. 2006).

Dimensionless parameters, such as the Reynolds Number and the Womersley Number, are matched with the respective parameters found in vivo flows and play an important role in producing physiologically representative fluid flows for use with PIV experimentation. Additionally, flow characteristics can be examined quantitatively and qualitatively to

verify that data from the PIV setup is appropriate as a basis for validating CFD, including:

1) verifying that the fluid flow upstream of the aneurysm in the parent artery has laminar flow conditions to make sure that the flow into the aneurysm is clean and uninfluenced by flaws in the model;

2) formation of Dean Vortices as associated with a curved artery (as used in the current study); and

3) inflow patterns consistent with previous in vitro and in vivo research.

These parameters were studied in a PIV experiment as focii for the current work. This PIV experiment was part of a larger study at Tohoku University, where other investigators were using CFD to study a model aneurysm similar to the experimental PIV model used in this study. The goal of the current study was to create a PIV setup that could be used to produce realistic hemodynamics for validation of future CFD data produced at Tohoku University.

METHODS AND MATERIALS

PIV experimentation and data collection were carried out during the summer of 2010 at Ohta Labs of Tohoku University in Sendai, Japan. The experimental setup consisted of a pulsatile flow system, which was configured to realistically reproduce conditions found in cerebral aneurysms. Hemodynamics were described using standard analytics, with a focus on observing primary and secondary flows associated with the model aneurysm.

Circulation System

A circulation system was set up that featured [Figure 1]:
  1) a settling tank;
  2) an impeller pump [Cyclo Drive, Sumitomo Heavy Industries Ltd., Model CNNM-4115-6] controlled by a laptop to transport a working fluid from a settling tank to the test section using a pulsatile waveform;
  3) a coriolis flowmeter [RotaMass, Yokogawa Corporation, Series 3] situated upstream from the test section so as to measure instantaneous flow rate through the circulation system;
  4) the cerebral aneurysm model; and

5) a damping tank located after the test section to absorb disturbances

and potential reflections in the pulsatile flow.

This setup was similar to that used by Krisztina Baráth to study the

influence stents have on intra aneurysmal hemodynamics (Baráth et al.

2005), except the flowmeter and damping tank were added to facilitate

pulsatile flow recording and development.


Working Fluid


Blood is a non-Newtonian fluid having a variable viscosity based on its

velocity; however, this property is significant only in small blood vessels

such as capillaries and artirioles (Ethier and Simmons 2007). For the

current experiment, the modeled intracranial blood vessel was of sufficient

size that a Newtonian fluid assumption could be made and viscosity

assumed constant.

The working fluid for the circulation system started as a mixture of

30 percent glycerol and 70 percent distilled water. Glycerol was then

added until the index of refraction of the working fluid matched that of the

silicone model, causing the mixture ratio to shift to approximately 35%

glycerol and 65% water. Matching the index of refractions minimizes the

distortion of light passing through the curved wall of the aneurysm and

artery within the model.  After the index of refraction matching was

performed, the working fluid had a kinematic viscosity of 3.74 micrometers

squared per second, a density of 1.094 grams per centimeter cubed and an index of refraction of 1.408.

Pulsatile Flow

Two dimensionless parameters were used to characterize the pulsatile flow: (1) the Reynolds Number

$$Re = \frac{V * D}{\nu}$$

where $Re$ = the Reynolds Number, $V$ = velocity (m/s), $D$ = diameter of the model artery (m), and $\nu$ = kinematic viscosity (m²/s)

and (2) the Womersley Number

$$\alpha = .5 * D * \sqrt{\frac{\omega}{\nu}}$$

where $\alpha$ = Womersley Number, $D$ = diameter of the model artery (m), $\omega$ = oscillatory frequency (Hz) and $\nu$ = kinematic viscosity (m²/s)

The Reynolds Number is a parameter that gives the ratio of inertial forces to viscous forces. The flow waveform was sinusoidal, with average bulk flow velocities ranging from 0.19 m/s to 0.41 m/s and Reynolds Numbers ranging from 200 to 430 [Figure 2]. The Womersley Number is a dimensionless parameter which describes the ratio between the inertial

forces caused by the pulsatile flow and the effects of viscosity. The flow had a frequency of one hertz and a Womersley Number of 1.03. Both dimensionless numbers were consistent with those typically found within blood vessels in the Circle of Willis (Ethier and Simmons 2007), which is a common area for aneurysms.

While the experimental setup and programmed waveform were designed to minimize the effects that damping and wave reflections had on the pulsed waveform, small discrepancies between the ideal waveform and the actual waveform were recorded by the flow meter at the apex of the pulses [Figure 2]. The PIV results during the discrepancies did not appreciably change.

PIV System

A PIV system was set up to capture images appropriate for PIV analysis [Figure 1]. The working fluid of the circulation system was seeded with spherical polymethylmethacrylate particles (Sekisui Tech Polymer MBX-20; Sekisui Plastics Co., Ltd.; http://www.tech-p.com/en/products/index.html#mbx) with a mean diameter of 17.41 microns and a specific gravity of 1.20. Planar illumination of the seeded particles within the model artery and aneurysm was produced using a 100 milliwatt Nd-YAG continuous laser beam passed through a cylindrical lens that created a light sheet with a nominal thickness of 1mm. The area of interest was

small enough that the relatively low powered continuous laser could adequately illuminate the particles, negating a need for a synchronizer as associated with a more powerful pulsed laser setup. The laser was fixed to a mount on a work bench, and the model was set on a three axis adjusting rig, which allowed movement of the model so that a variety of different planes could be illuminated. Thirteen planes in total were recorded, five along the x axis, five along the y axis, and three along the z axis situated across the aneurysm orifice [Figure 3].

A laptop controlled a Photron Fastcam high-speed camera (Fastcam, SA-3, Photron, Japan; www.photron.co.jp), which captured bitmap images of the particles illuminated by the laser sheet. Up to five gigabytes of continuous images could be temporarily stored on the camera's internal memory before having to transfer the data over to an external hard drive. This allowed for continuous photographs of three full wave pulses over approximately three seconds at 2000 frames per second for each plane view, providing a time difference of 500 microseconds between consecutive images.

Model Aneurysm

A block of silicone was molded into a model curved artery with a saccular aneurysm attached at a 90 degree angle to the bend [Figure 4]. Silicone's transparency and elasticity is ideal for PIV analysis in cardiovascular

studies, allowing the working fluid to pass through in visible and physiologically realistic ways (Augsburger et al. 2009).

Early PIV research investigated hemodynamics and how they changed with geometric variations of the aneurysm alone and set up on a straight parent artery (Liou et al. 1997), providing only primary flow effects. As models became more complex, the effects of parent artery geometry variations were incorporated into research, producing secondary flow effects within the model. Since cerebral aneurysms are commonly associated with curved arteries in one way or another, more complex models (various curvatures versus straight) are needed to better learn about hemodynamics. Aneurysmal flow of an aneurysm on a straight parent artery is primarily a shear-driven process, whereas flow through an aneurysm on a curved parent artery is primarily an inertially-driven one (Meng et al. 2006). This creates significantly different intra-aneurysmal flow conditions. While aneurysm circumferential position has little to do with the hemodynamics of aneurysms on straight parent arteries, it has been found to cause large shifts and changes in flow structures within aneurysms on a curved parent artery (Liou et al. 2006). In a CFD study, Sato et al. (2007) varied aneurysm geometry as well as changing circumferential position of the aneurysm on a curved parent artery and found that aneurysm placement on a curved artery had the most effect on intra-aneurysmal flow. Additionally, they found that aneurysmal flow in an aneurysm which is situated at a 90 degree angle to the bend in a parent

artery experienced a larger aneurysm inflow than at 0 or 180 degrees to the bend. It was this study and result in particular that was the impetus for current thesis work and use of PIV experimentation on a curved artery model with an aneurysm attached at 90 degrees at/to the bend.

The model for the current study had an artery inner diameter of 4 mm, a radius of curvature of 6mm and a perfectly spherical aneurysm with an inner diameter of 4mm. The coordinate axis origin for the model aneurysm was chosen to be at the center of the aneurysm orifice, with the x axis running perpendicular to the flow in the parent artery, the y axis running toward the top of the aneurysm, and the z axis going downstream.

In order to obtain a fully developed flow state before reaching the curved portion of the model during pulsatile flow, the flow had to be designed to go through a straight tube length, with minimum length defined as follows (Womerseley 1955):

$$L = .06 * D * Re$$

where $L$ = minimum length (m), $D$ = diameter of the artery (m) and $Re$ = Reynolds Number.

For the model parent artery with an inner diameter of 4mm and maximum Reynolds Number of 430, a straight section of approximately 10 centimeters is required in order to reach laminar flow conditions before the fluid reaches the curved section of the artery. This development of laminar flow is an integral part of verifying that the PIV setup was functioning properly and therefore could be used to validate subsequent CFD results.

Software

A LabView (National Instruments, http://www.ni.com/labview/) user interface was set up for simultaneous triggering of the high speed camera recording and recording of flow rate data from the coriolis flow meter. LabView recorded the time and flowrate in milliliters per second at 2000 hertz to match the recording rate of the Photron Camera. The high-speed camera was directly controlled with the Fastcam viewer interface downloaded from the Photron website (www.photron.com). It allowed for control over the camera parameters, such as frame rate and shutter speed, as well as the fine tuning of many variables, such as contrast and gain, so that a well-defined image of the particles and the flow field could be developed.

Images obtained with the PIV setup were transported to Syracuse University and uploaded into the PIV analysis program FlowManager (Dantec Dynamics, Ver. 4.71.05, 2006). The images were calibrated with an image taken of a ruler in the laser plane. A mask was applied to black out areas outside of the aneurysm, which could add unwanted background signals. An adaptive cross-correlation technique was applied to the images. This technique involved several sweeps of a pair of consecutive images, breaking the images up into interrogation areas, with each sweep involving smaller interrogation areas. Signal processing was then used to

compare the interrogation areas of the consecutive images so that displacement of the particles within an interrogation area could be found. This displacement was combined with the time difference in the images so that a velocity could be given at the original interrogation area. The initial sweep was with interrogation areas of 32 pixels by 32 pixels and the final sweep had an interrogation area of 16 pixels by 16 pixels and an overlap of 50 percent. This final sweep size correlates with a PIV resolution of 64 by 32 (vectors in the velocity field) and a rough average of 7-10 particles per interrogation area [Figure 5].

Velocity in the parent artery in the direction of bulk flow was higher than that in the aneurysm. In order to keep the particles from blurring in the parent artery, the shutter speed was increased to 1/7500 of a second (frame rate was held constant at 2000 hertz). The increased shutter speed caused the contrast between the particles and background noise to decrease and preprocessing was required before the images could be analyzed with the PIV software. Adobe Photoshop's (Adobe, Version CS5; www.adobe.com) batch processing technique was used to apply contrast and noise filters where required.

The final PIV data breaks a pulse into six time steps. The final velocity fields for each time step represent the phase averaged velocities of 10 milliseconds of data over several pulse cycles.

Verification of Flows in the Experimental System

Several structures and characteristics of the flow within the model parent artery and aneurysm were examined to verify that the experiment was set up correctly and producing hemodynamics that were realistic, and therefore useful.

*Laminar Flow*

Flow upstream from the aneurysm was imaged and expected to show characteristics of being laminar, characterized by a parabolic velocity profile spanning the width of the artery [Figure 6] (Munson et al. 2006). The profile is dictated by the equation for laminar flow in a pipe:

$$\frac{V_r}{V_{Max}} = 1 - \frac{r^2}{R}$$

Where $V_r$ = velocity at a distance $r$ (m/s), $V_{Max}$ = velocity at center of pipe (m/s), $r$ = radial distance from center (m), $R$ = radius of the pipe (m).

A clean incoming flow assures that the flow characteristics seen in the data collected from the experimental setup are caused by the geometry of the aneurysm and parent artery and not by unintended disturbances, such as the effects from the tubes connecting the flowmeter to the model.

*Dean Vortices*

In curved parent arteries, centrifugal forces cause Dean Vortices to form. These counter-rotating pairs of vortices were first described as a phenomenon of curved pipes (Dean 1928). Dean Vortices can greatly influence the velocity in and around an aneurysm. Inertial effects cause fluid flowing at the center of the pipe to develop a velocity component perpendicular to the bulk flow going toward the outside of the bend. This causes fluid at the outside bend of the pipe to be displaced outwards along the curvature of the pipe toward the inside of the bend. The model flow was expected to have a Dean Vortex secondary flow, creating increased intra aneurysmal flow [Figure 7]. These Dean Vortices are seen by taking images in the aneurysm region perpendicular to the bulk flow, in what was designated as the XY plane.

*Inflow Characteristics of Aneurysm Orifice*

The inflow at the aneurysm orifice is an important characteristic both for CFD validation purposes and in designing effective endovascular structures, such as stents and embolization coils (Imai et al. 2008). High velocity inflow is expected at the outside bend of the aneurysm. and a slower larger area of outflow is expected in the central and inside bend of the aneurysm.

19
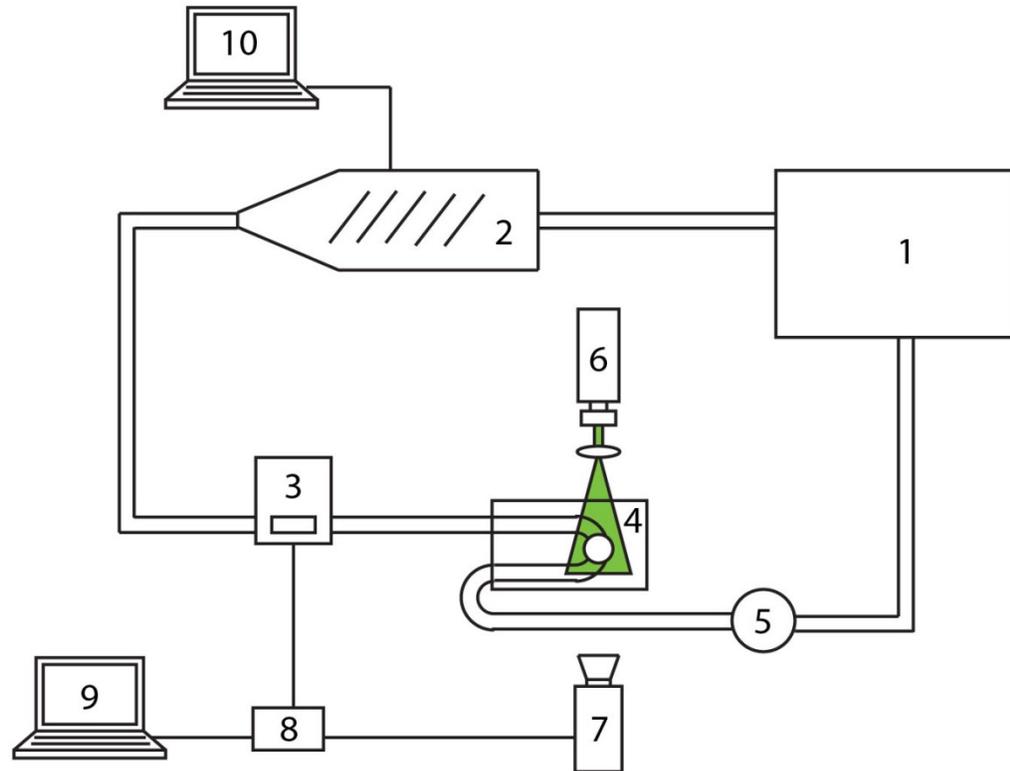


**Figure 1 – Experimental Setup – The experimental system consisted of a circulation system and periphery equipment used in Particle Imaging Velocimetry (PIV) analysis. These included: 1) Settling Tank; 2) Impeller Pump; 3) Coriolis Flowmeter; 4) Model Aneurysm; 5) Damping Tank; 6) Laser and Cylindrical Lens; 7) High Speed Camera; 8) LabView Interface Connection; 9 and 10) Laptops controlling the PIV system and impeller pump, respectively.**
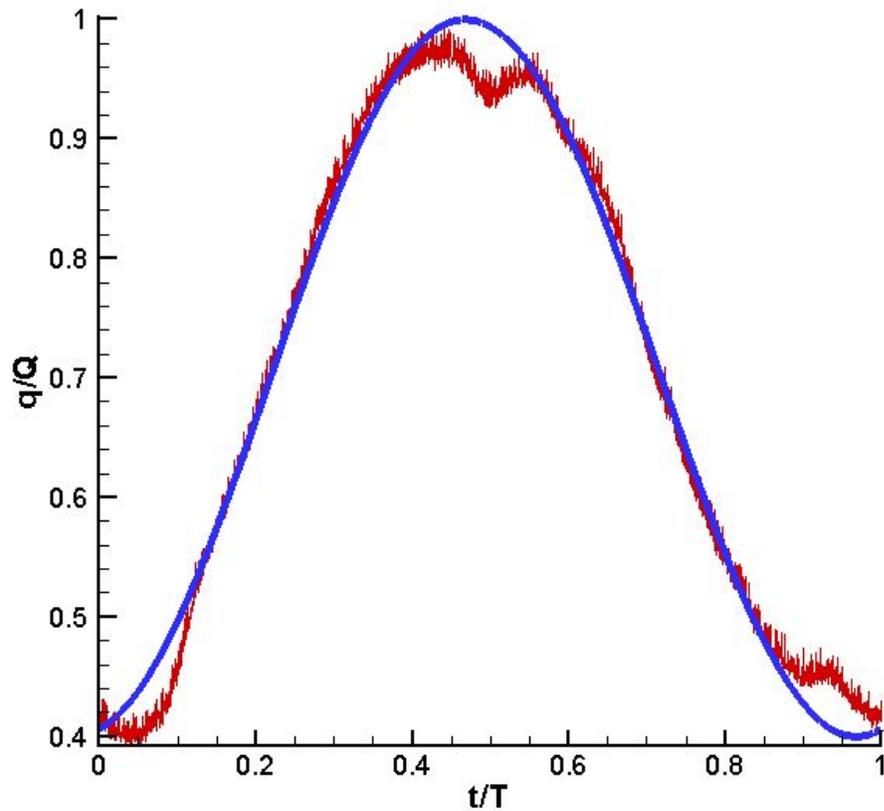
**Figure 2 – Pulsatile Waveform – Unavoidable reflections and damping within the experimental setup caused the actual experimental waveform, as recorded by the coriolis flowmeter (red data), to deviate from the ideal sinusoidal waveform (blue line). Normalized flow is plotted against the normalized time step for one waveform.**
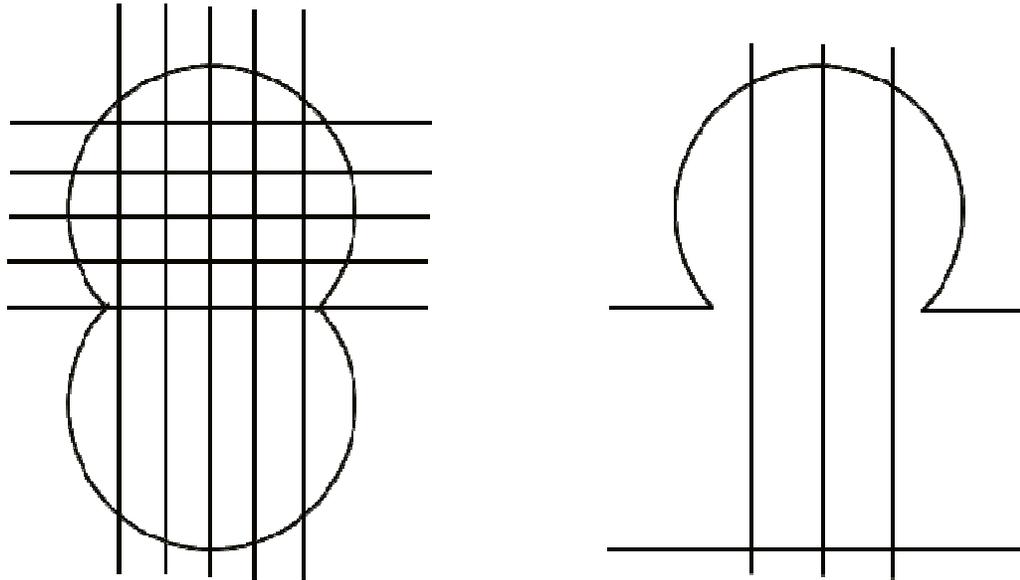
**Figure 3 – Imaging Planes – Thirteen imaging planes were recorded with the use of the Particle Imaging Velocimetry (PIV) setup. The origin for the coordinate system used was at the center of the aneurysm orifice, with five imaging planes along the x-axis, five along the y-axis, and three along the z axis.**
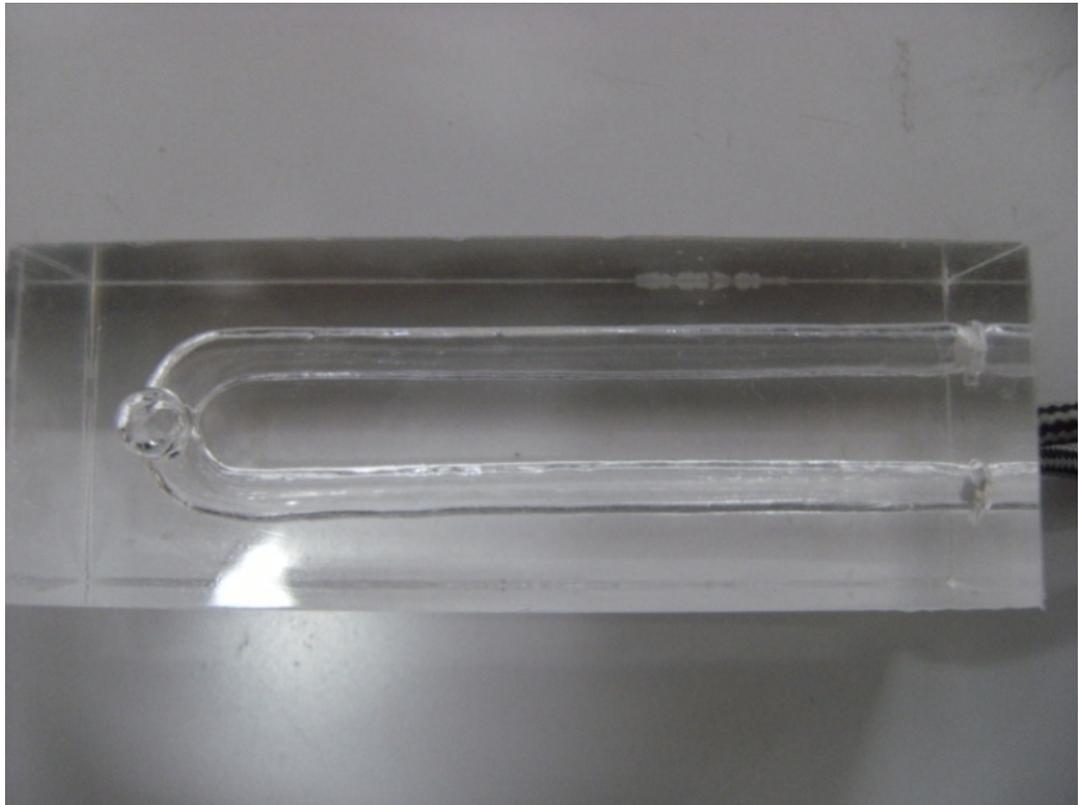
**Figure 4 – Aneurysm Model – I chose to study an aneurysm arising on the lateral side of a curved parent artery. The model was constructed out of silicone, which has been shown to have a response similar to arterial tissue and is conducive to Particle Imaging Velocimetry (PIV) analysis due to its transparency. The inner diameter of the aneurysm and parent artery was 4mm, and the radius of curvature was 6mm.**
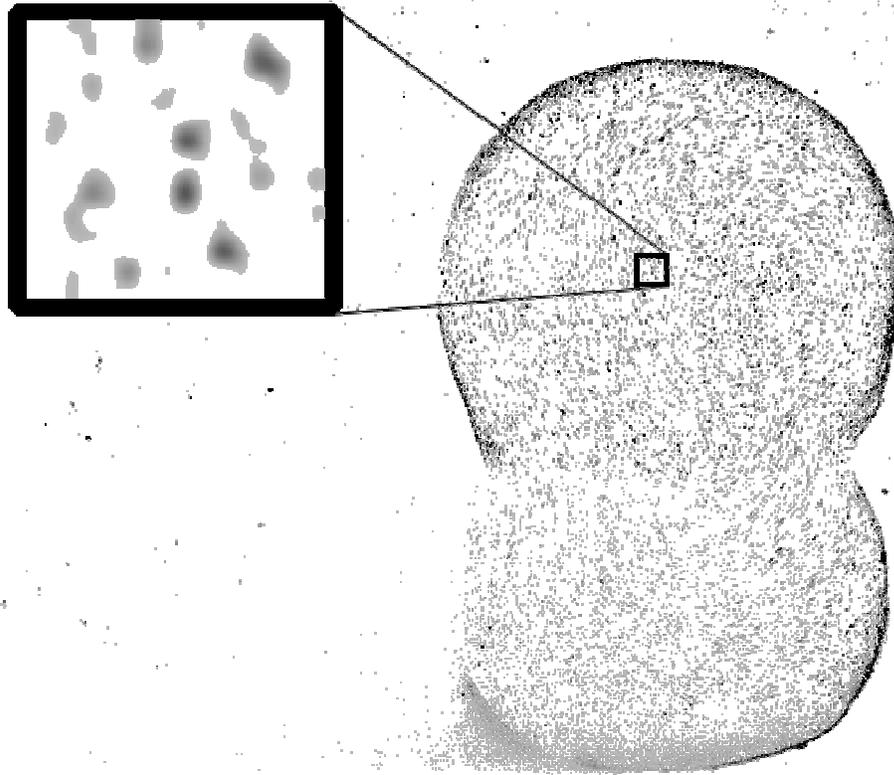
**Figure 5 – Particle Imaging Velocimetry (PIV) Interrogation Area – PIV analysis uses signal processing to correlate interrogation areas from two different images so that velocity fields can be produced. In order to produce good results, seven to ten particles should be within each interrogation area (see square insert). This was achieved with a final interrogation area of 16 pixels by 16 pixels.**
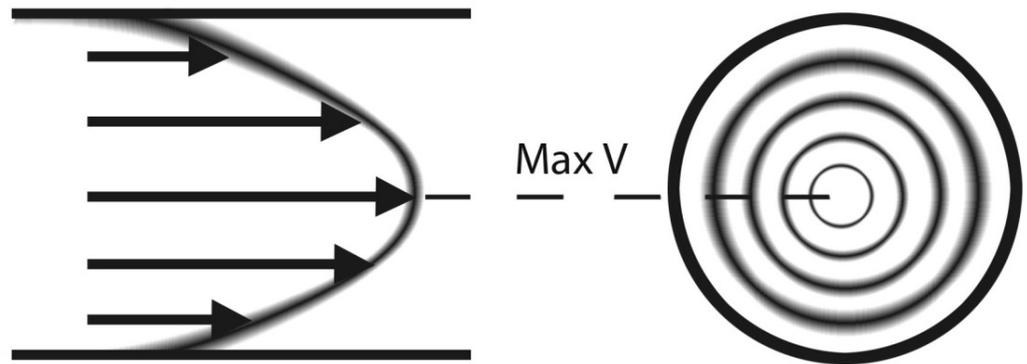
**Figure 6 – Expected Laminar Flow in a Pipe – A parabolic flow profile develops across an uninfluenced laminar flow in a pipe or an artery modeled as a pipe. The maximum flow velocity (Max V) is achieved at the center of the pipe, and the outer edge of the flow achieves a no slip condition where velocity is zero.**
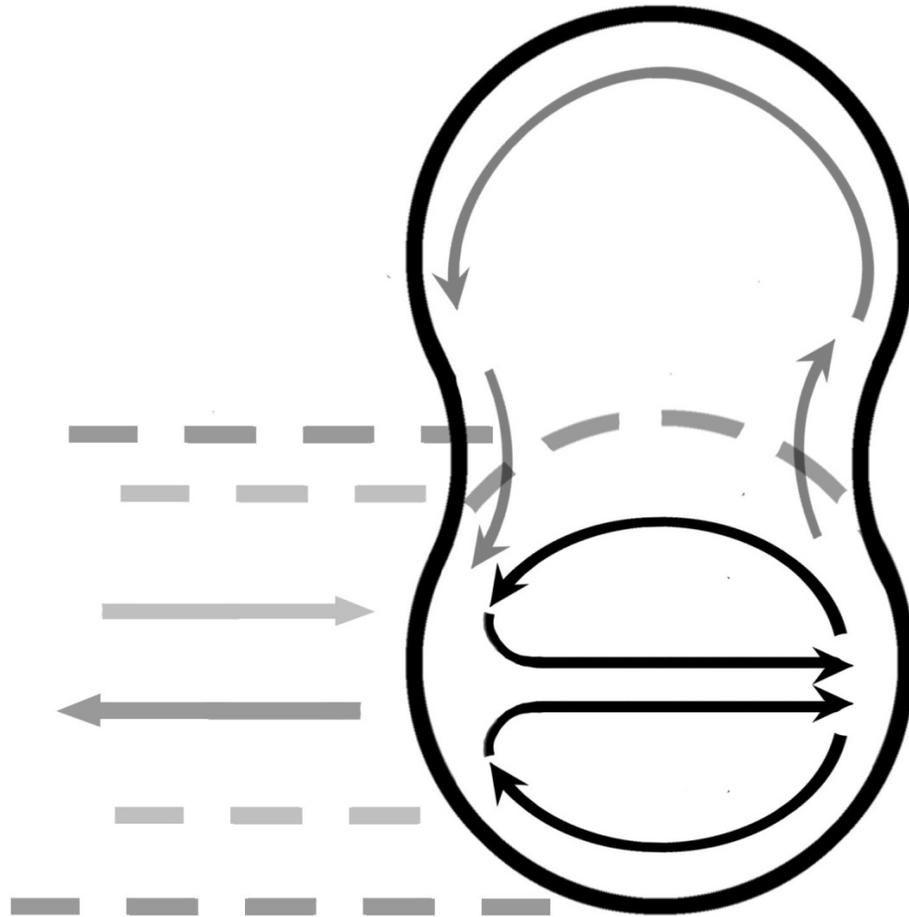
**Figure 7 – Expected Qualitative Flow within Aneurysm Model – Flow structures of the aneurysm and near aneurysm region in the central plane perpendicular to bulk flow in the parent artery where Dean Vortices have developed in the parent artery. Flow in this plane is primarily inertially driven, caused by the curvature of the parent artery.**

RESULTS

With the goal of this work being the creation of a database of flow information collected from PIV experimentation analysis for validation of future CFD work, it was important to verify that the experimental system had been set up under the correct specifications and that usable data which accurately portrayed the physiological system was collected. This was accomplished by checking the flow parameters and the upstream flow profile, and checking that the flow structures corresponded with physiological structures of in vivo flows.

Laminar Flow

A parabolic flow profile was observed in the model artery section upstream from the aneurysm cavity, consistent with a laminar flow condition [Figure 8]. This profile was produced during the systolic phase of the pulsatile waveform. Resolution and near wall effects prevented measurements close to the arterial wall, but the flow profile indicates that it approaches a no slip condition. The flow had an average speed of 0.33 meters per second, corresponding to a Reynolds number of 355.

The parabolic flow profile found upstream of the model aneurysm confirms that laminar flow developed in the working fluid before it reached the curved section of the model. Because of this, it can be inferred that the

data collected to form the database for CFD verification is a product of only the model's geometry.

Secondary Flow and Dean Vortices

Two distorted asymmetric counter-rotating secondary flows known as Dean Vortices were observed to form perpendicular to the bulk flow in the parent artery [Figure 9]. The lower Dean Vortex was reduced in size, residing in the bottom two-fifths of the parent artery, with its center slightly shifted towards the outside of the curvature at x = 0.5 mm. The upper Dean Vortex expanded and was distorted to fill the entire region of the aneurysm and approximately three-fifths of the parent artery, with its center shifted towards the outside of the curvature of the parent artery at x = 0.8 mm.

Aneurysm Inflow

It was observed that approximately 25 percent of the aneurysm orifice consisted of inflow at an average velocity of 0.09 meters per second, and 75 percent of the aneurysm orifice consisted of outflow at an average speed of .023 meters per second [Figure 10]. The inflow was found to qualitatively compare well with Imai et al.'s (2008) previous work with the inflow of aneurysms on a curved parent artery.

Database

PIV data was collected from 13 planes at six different times evenly spaced over one pulse cycle of the transient flow. All of the one millimeter thick planes complement each other to provide information on the entire aneurysm and near aneurysm region of the parent artery from three different viewpoints for use in future CFD verification.

The sum of the contributions of primary and secondary flow within the model caused a helical structure to form within the aneurysm. Flow entered the aneurysm through the positive x positive z quadrant of the aneurysm orifice, crossed the dome of the aneurysm diagonally, and primarily exited through the negative x negative z quadrant.
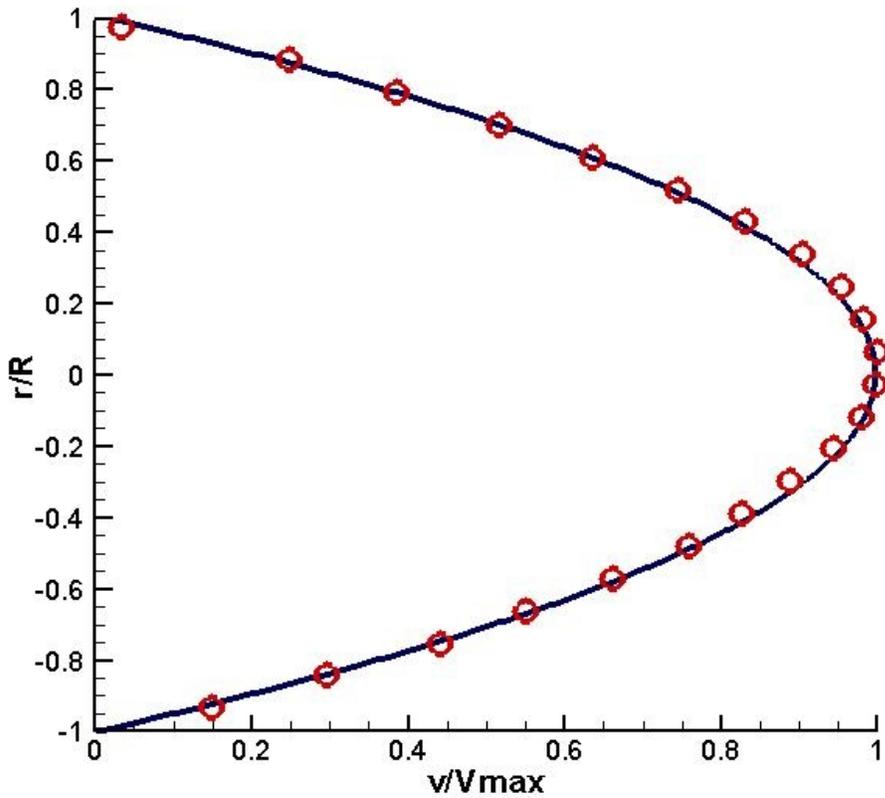
**Figure 8 – Laminar Flow in the Parent Artery – A laminar flow
condition was achieved in the upstream straight portion of the parent
artery, indicating that the flow is uninfluenced by sources outside of
the silicone model. The normalized velocity, plotted on the horizontal
axis, is dependent on the normalized radius, plotted on the vertical
axis, with red circles representing observed velocity points acquired
with PIV analysis plotted against an ideal laminar flow profile.**
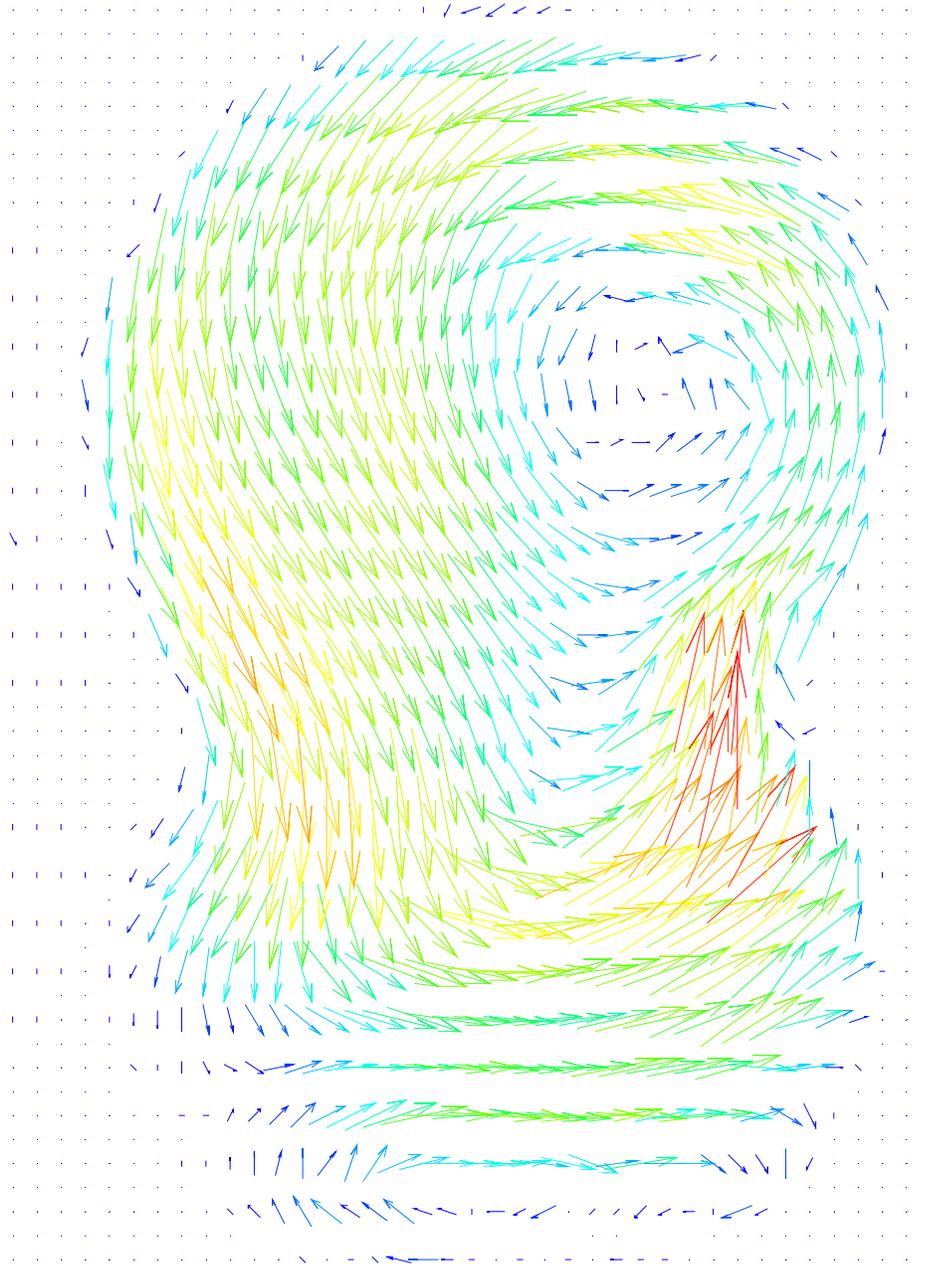
**Figure 9 – Secondary Flow – A secondary flow structure consisting of two counter-rotating vortices, known as Dean Vortices, was observed. The upper vortex has deformed and expanded to fill the aneurysm and a large portion of the parent artery. Vectors representing the flow range from short blue arrows, indicating low-speed regions, to long red arrows, indicating high-speed regions.**
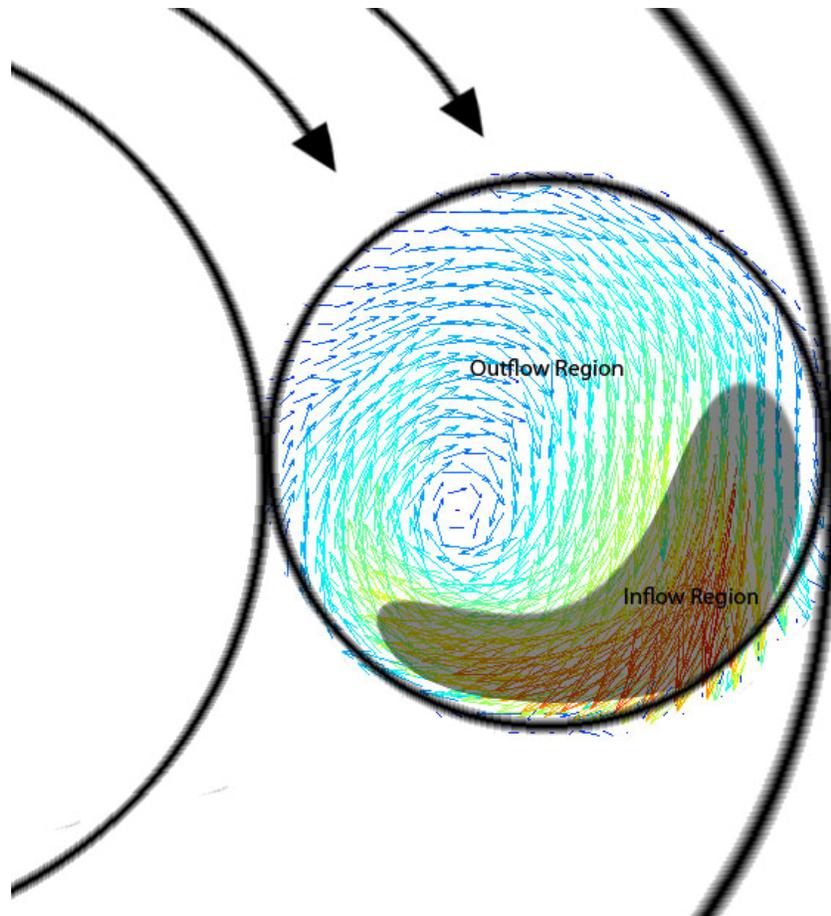
**Figure 10 – Aneurysm Inflow – Fluid flowed into the aneurysm through the quadrant that was downstream and on the outside of the arterial bend and flowed out primarily in the quadrant that was upstream and on the inside of the arterial bend. Vectors representing the flow range from short blue arrows, indicating low-speed regions, to long red arrows, indicating high-speed regions.**

DISCUSSION

Computational Fluid Dynamic modeling has the prospect of greatly improving the ability to accurately and quickly diagnose risks associated with an aneurysm based upon the hemodynamic effects of different geometric configurations. If this technique is going to make improvements in such diagnoses, complex models that mimic cerebral arteries and aneurysms are needed, and CFD results must be validated for accuracy. Results presented in this Honors Thesis are one step toward the validation of CFD aneurysm modeling. A database of flow velocities was created from PIV analysis of a silicone model simulating a cerebral aneurysm situated at a 90 degree angle to a curvature in a parent artery. The database includes flow details and contains information over the entirety of the aneurysm and near aneurysm region under pulsatile flow conditions, which will prove useful in the validation of complex transient flows.

This work supplements previously published works on cerebral aneurysms arising from curved parent arteries. The flows found in this experimental setup show significantly different secondary flow patterns than those found with the use of PIV and CFD analysis carried out by Liou et al. (2006). They explored a number of different circumferential aneurysm positions with a model which had a slightly smaller parent artery and larger aneurysm. Their 90-degree angle aneurysm under similar

conditions contained three vortices, one in the aneurysm, one in the orifice, and one at the bottom of the parent artery. In contrast, observations in the current study were of only two vortices, one large vortex in the aneurysm that extended into the artery, and the other small vortex below. One possible cause of this is that the difference between Liou et al. and the current study could be due to aneurysm dimensions: the Liou et al. model was not perfectly spherical, with an aneurysm diameter that was one and a half times the parent artery diameter and a height that was two times the diameter of the parent artery. In the current study, the aneurysm was perfectly spherical, with a diameter that was the same as the width of the artery – 4 mm each. It has been shown that aneurysms with a high aspect ratio can present with an additional counter-rotating vortex in the tip of the aneurysm (Ujiie et al. 1999).

A steady state CFD study carried out by Sato et al. (2007) produced results that are consistent with the flow structures found in the model aneurysm of this experiment, but no data was provided for regions outside of the aneurysm, and it contained no data on pulsatile flow (Sato et al. 2007). Although a CFD model of the exact proportions of the aneurysm found in this experiment has not yet been completed by Ohta Labs, results from a model of the same configuration but with a spherical aneurysm which has a diameter twice that of the parent artery shows apparent agreement, with two vortices in approximately the same positions as in the current experiment, but with the lower vortex being

more distorted toward the outside wall of the parent artery [Figure 11]. This is more evidence to support the conjecture that the aspect ratio is the impetus for the third vortex in the Liou et al. study.

The database constructed in the current study will be helpful in validation of a narrow range of the complex aneurysms currently undergoing research with similar geometric parameters. With Liou et al.'s (2006) previous results on similar aneurysms resulting in different flow structures, these results may help guide future research into why there were these variations in the results. CFD analysis could then be explored to see if they exhibit the same trends.

The results of this experimentation were limited in some ways by the resources at disposal. There were several concessions which had to be made when designing the experimental setup. The impeller style pump utilized in the experiment was not the most ideal pump for creating physiologically similar and complex pulses. A positive displacement pump would have improved the control over the transient flow and could have produced more interesting and possibly more useful results. Additionally, the small area of interest of the aneurysm (at most four millimeters by eight millimeters) would have benefitted from a camera lens, which could have focused images at a closer distance, allowing the area of interest to fill more of the camera image. This would have allowed more particles to be seeded into the flow and a greater resolution to be produced from the PIV analysis.
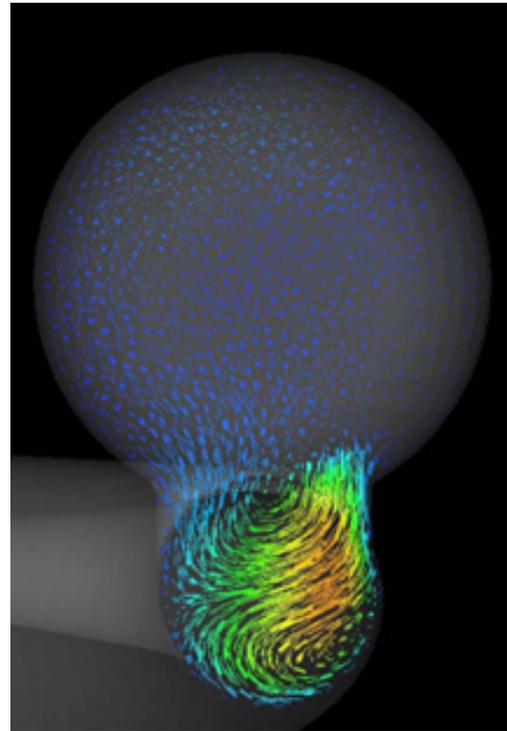
If the experiment was to be repeated, increased knowledge and experience would lead to several improvements upon the existing setup. One of the largest shortcomings of the project is the lack of utilizing a method for finding the wall shear stresses of the aneurysm. The wall shear stress, as well as other parameters that can be derived from it, have been found to be among the most important indicators in aneurysm rupture prediction. Standard PIV image capturing fails to produce data in the near wall region needed for the resolution of wall shear stresses because of particle density, light refraction, and near wall disturbance problems (Goldstein 1996). Special techniques can be used to find this data if they are prepared for in the setup of the experiment. While the overall goal of CFD validation is largely satisfied with the flow velocity data produced in the current study, the wall shear stresses would have been a valuable supplement to the existing database. A view of the Dean Vortex in the parent artery upstream from the aneurysm also may have provided some interesting insights as to the development of the flow, as well as helped verify initial flow conditions within the curved parent artery.

SUMMARY AND CONCLUSION

A viable PIV experimental setup was developed that produced realistic

hemodynamics in a model curved parent artery with an aneurysm arising

at a 90 degree angle to the bend as a basis for validating future CFD

work. Thirteen imaging planes were analyzed at six different times during

a sinusoidal pulsatile flow. Laminar flow, Dean Vortices, aneurysmal inflow

and other details were scrutinized to verify that the data collected was an

accurate representation of a simplified in vivo cerebral aneurysm.

Verification of the realistic flows through the experimental setup means

that data collected is appropriate to validate CFD data on similar models.
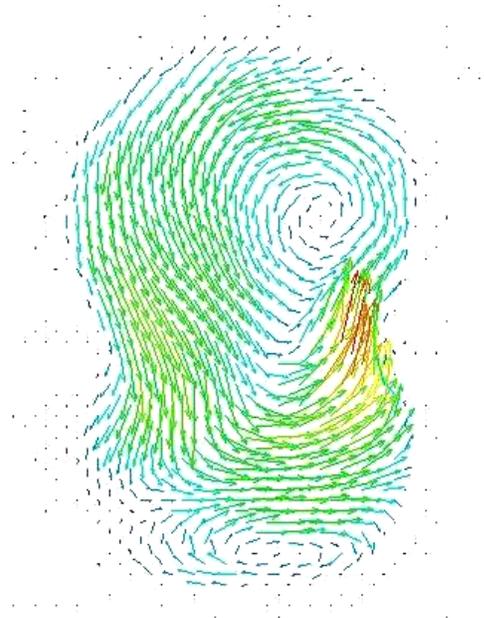
A. PIV from the current study          B. CFD from Ohta Labs, Japan

**Figure 11 – PIV and Preliminary CFD Velocity Fields – The PIV results in the plane z=0, shown to the left of the figure (A), has similar flow structures to the CFD results from an aneurysm with similar geometric parameters (B) (CFD image courtesy of Ohta Lab). An exact CFD model is still being developed at Ohta Lab. Vectors representing the flow range from short blue arrows, indicating low-speed regions, to long red arrows, indicating high-speed regions.**

LITERATURE CITED

Augsburger L, P Reymond, E Fonck, Z Kulcsar, M Farhat, M Ohta, N Stergiopulos, D Rufenacht. Methodologies to Assess Blood Flow in Cerebral Aneurysms: Current State of Research and Perspectives. *Journal of Neuroradiology*, 2009; 36(5): 270-277.

Baráth K, F Cassot, J Fasel, M Ohta, D Rufenacht. Influence of Stent Properties on the Alteration of Cerebral Intra-Aneurysmal Haemodynamics: Flow Quantification in Elastic Sidewall Aneurysm Models. *Neurological Research*, 2005; 27: 120-128.

Brisman J, J Song, D Newell. Cerebral Aneurysms. *The New England Journal of Medicine*, 2006; 355(9): 928-939.

Cebral J, F Mut, Jane Weir, C Putnam. Association of Hemodynamic Characteristics and Cerebral Aneurysm Rupture. *Journal of Neuroradiology*, 2010; 32(2): 264-270.

Chen P, K Frerichs, R Spetzler. Current Treatment Options for Unruptured Intracranial Aneurysms. *Neurosurgery Focus*, 2004; 17(5): 1-6.

Dean W. The Streamline Motion of Fluid in a Curved Pipe. *Philosophical Magazine*, 1928; 5: 673-695.

Ethier C, C Simmons. *Introductory Biomechanics: From Cells to Organisms*. Cambridge University Press, New York, 2007.

Goldstein R. *Fluid Mechanics Measurements, Second Edition*, Taylor and Francis, Washington DC, 1996.

Hoi Y, S Woodward, M Kim, D Taulbee, H Meng. Validation of CFD Simulations of Cerebral Aneurysms with Implication of Geometric Variations. *Journal of Biomechanical Engineering*, 2006; 128(6): 844-851.

Imai Y, K Sato, T Ishikawa, T Yamaguchi. Inflow into Saccular Cerebral Aneurysms at Arterial Bends. *Annals of Biomedical Engineering*, 2008; 36(9): 1489-1495.

ISUIA (International Study of Unruptured Intracranial Aneurysms) Investigators. Unruptured Intracranial Aneurysms – Risk of Rupture and Risks of Surgical Interventions. *New England Journal of Medicine*, 1998; 339(24): 1725-1733.

Juvela S. Prehemorrhage Risk Factors for Fatal Intracranial Aneurysm Rupture. *Journal of the American Heart Association*, 2003; 34:1852-1858.

Liou T, W Chang, C Liao. LDV Measurements in Lateral Model Aneurysms of Various Sizes. *Experiments in Fluids*, 1997; 23(4): 317-324.

Liou T, Y Li, W Juan. Numerical and Experimental Studies on Pulsatile Flow in Aneurysms Arising from a Curved Parent Vessel at Various Angles. *Journal of Biomechanics*, 2006 40(6): 1268-1275.

Meng H, Z Wang, M Kim, R Ecker, L Hopkins. Saccular Aneurysms on Straight and Curved Vessels Are Subject to Different Hemodynamics: Implications on Intravasvular Stenting. *American Journal of Neuroradiology*, 2006; 27(9):1861-1865.

Munson B, D Young, T Okiishi. *Fundamentals of Fluid Mechanics Fifth Edition*. John Wiley and Sons Inc., New York, 2006.

Raffel M, C Willert, J Kompenhans. *Particle Image Velocimetry: A Practical Guide*. Springer Berlin, 1998.

Sato K, Y Imai, T Ishikawa, N Matsuki, T Yamaguchi. The Importance of Parent Artery Geometry in Inra-aneurysmal Hemodynamics. *Medical Engineering and Physics*, 2007; 30(6): 774-782.

Shimogonya Y, T Ishikawa, Y Imai, N Matsuki, T Yamaguchi. Can Temporal Fluctuation in Spatial Wall Shear Stress Gradient Initiate a Cerebral Aneurysm? A Proposed Novel Hemodynamic Index, the Gradient Oscillatory Number (GON). *Journal of Biomechanics*, 2009; 42: 550-554.

Taylor C, M Draney. Experimental and Computational Methods in Cardiovascular Fluid Mechanics. *Annual Review of Fluid Mechanics*, 2004; 36: 197-231.

Ujiie H, H Tachibana, O Hiramatsu, A Hazel, T Matsumoto, Y Ogasawara, H Nakajima, T Hori, K Takakura, F Kajiya. Effects of Size and Shape (Aspect Ratio) on the Hemodynamics of Saccular Aneurysms: A Possible Index for Surgical Treatment of Intracranial Aneurysms. *Neurosurgery*, 1999; 45: 119-129.

Versteeg H, W Malalasekra. *An Introduction to Computational Fluid Dynamics: Finite Volume Method, Second Edition*. Prentice Hall, New York, 2007.

Waite L, J Fine. *Applied Biofluid Mechanics*. McGraw-Hill, New York, 2007.

Womerseley J. Method for the Calculation of Velocity, Flow Rate, and Viscous Drag in Arteries When the Pressure Gradient is Known. *Journal of Physiology*, 1955. 127(3): 553-563.